AN ULTRA-HIGH SPEED MULTI-SPARK CAMERA OF A PULSE-CONTROL TYPE

Takahashi, Kiyoshi
Research Institute for Applied Mehanics, Kyushu University : Associate Professor

Mada, Toshio
Research Institute for Applied Mechanics, Kyushu University

https://doi.org/10.5109/6776448

出版情報：Reports of Research Institute for Applied Mechanics. 28 (89), pp.21-34, 1980-12. 九州大学応用力学研究所
バージョン：
権利関係：

Reports of Research Institute for Applied Mechanics
Vol. XXVIII, No. 89, 1980

AN ULTRA-HIGH SPEED MULTI-SPARK CAMERA OF A PULSE-CONTROL TYPE

By Kiyoshi TAKAHASHI* and Toshio MADA**

A multi-spark camera of a pulse-control type has been constructed (RIAM-MC1). Typical performance of the camera is as follows: number of frames=24, maximum framing rate=1×10^6 frames/s, full width at half-maximum duration of a light pulse=0.4 μs, maximum energy of discharge capacitor=2 joules, light sourced dimension=1 mm, and static spacial resolution=6 lines/mm. Several examples of photography using the camera have been included, related to cavitation and wave propagation in water, fracture shadowgraphy of polymeric material and water eruption due to an under-water spark.

Key words: Multi-spark camera, Pulse-control type, High-speed photography

1. Introduction

High speed photography is a powerful means for observation of high speed phenomenon such as combustion, instantaneous deformation and fracture in solids, cavitation in liquids, and propagation of waves in fluids as well as in solids. There have been constructed various types of photographic systems, which have been used in a variety of speed ranges. Among them the following four types have been available for "ultra-high" speed uses: (1) high speed framing cameras (such as Beckman and Whitley), (2) high speed streak cameras with sequentially modulated laser light sources[1], (3) image converter cameras, and (4) multi-spark (or Cranz-Schardin[2]) cameras. Each has its own merits and demerits. However, the most conspicuous feature, and one common to all, is that they are too expensive to be easily obtained. Usually the total cost for one system amounts to ¥20, 000, 000, and it is not unusual for the cost to go well over ¥30, 000, 000.

The purpose of the present work is to construct an "ultra-high" speed camera for use in observation of various dynamic phenomena such as stated above. There were various requirements imposed on the present laboratory

* Associate Professor, Research Institute for Applied Mehanics, Kyushu University
** Research Institute for Applied Mechanics, Kyushu University

construction. First, because the reason for the present trial-construction lay in the high cost of the commercially available facilities, the camera must have excellent cost performance. Furthermore, it must be portable, so as to make its use outside the laboratory practicable. It must also be constructed without special knowledge of optics and optical techniques, and should be easily operated at negligible operation cost. The only type which seemed to be in accord with our requirements was the multi-spark type camera.

In connection with the framing-rate control method, that of the multi-spark camera may be classified into two types; one is the L-C* line type which was originally developed by Cranz and Schardin[2]. The other is the pulse-controlled type[3], which is an improvement over the Cranz-Schardin camera. In the case of the former, the framing rate is determined by the resonance frequency of a CLC loop. Usually, with fixed capacitance C, the resonance frequency is controlled by varying the inductance L. Consequently, this type has a drawback in that it lacks versatility in timing; usually the framing rate is limited to a high range, typically 30,000~800,000 frames/s. However, because the CLC loops are very simple, the control circuit does not cost so much as the pulse-controlled type. In the case of the latter, the framing rate is determined by a clock pulse circuit, so that there is no lower limit imposed on the rate (as for the upper limit, see **3. 6**). This makes it possible for us to employ the camera in a much wider range of uses than was possible with the former type. The framing rate may be easily changed by manual setting of the clock pulse interval on a circuit panel. However, because the control circuits should contain a number of low voltage IC-circuits for the sake of compactness of the apparatus, protection of the circuits against severe electromagnetic perturbations due to spark discharges should by all means be planned for; but this is not always technically easy.

Nevertheless, for the sake of a greater range of applications, we preferred to construct the pulse-control type apparatus described in the present work**.

2. Principle and design of the multi-spark camera

Figure 1 illustrates the basic principle of the present multi-spark camera, where G is a spark gap for a light pulse source, M is a concave reflector, S is the specimen, L is a lens and F is film sheet. (Instead of the reflector one can also use a field lens, such as a Fresnel lens, which would be placed between S and L on the straight light path of G-S-L-F[2].) The light from G is collected by M (or the field lens) and is focused on L. Because

* L and C stand for inductance and capacitance, respectively.

** As far as we know, neither commercially nor in an in-laboratory manner has such an apparatus with so many frames been constructed in Japan. The present apparatus has been given the nickname of RIAM-MCl after the name of the Institute.

each of the spark lights is focused on a particular lens which corresponds to a particular gap, and because each is fired in succession at a pre-determined interval, it is possible to obtain time-sequential separate images of a specimen model on a film plane; the present apparatus has 24 gaps and the same number of lenses, each squarely arrayed, so that 24 images in one time-controlled sequence may be obtained.

Figure 2 is a block diagram of the control pulse circuits connected to the spark discharge circuits. (Two of the twenty-four channels are shown.) Firing of G is initiated by breakdown of a trigger gap TG, whose electrodes are made of thick aluminum plates spaced approx. 3 mm apart in an air atmosphere. A system of pulse circuits was designed and constructed to obtain multi-channel high voltage pulses which trigger the trigger gaps (TG_1~TG_{24}) successively at a predetermined rate. As is shown in Fig. 2, this system consists of a gate trigger pulse circuit (GTPC), a clock pulse circuit

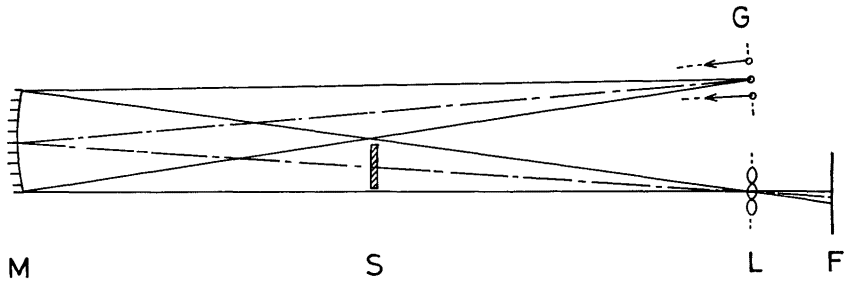

Fig. 1 Principle of the multi-spark camera.

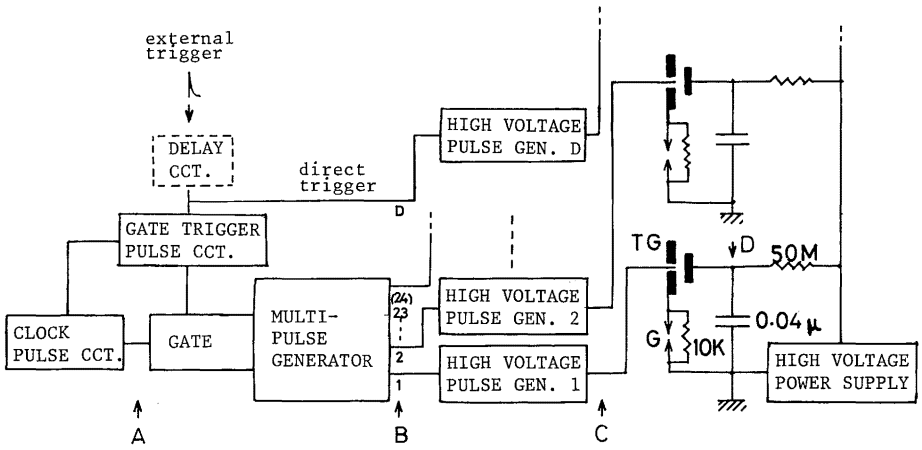

Fig. 2 Block diagram of the control pulse circuits, which are connected to the spark discharge circuits.

(CPC), a multi-channel pulse generator (MPG) with a gate and multi-channel high voltage pulse generators (HVPG). Occasionally, when synchronization with an event to be observed is necessary, a delay circuit (DC) is used in advance of the GTPC. In the ready mode, the GTPC is set into operation either internally by manual action or externally by an external synchronizing trigger pulse. Clock pulses from the CPC are only transmitted to the MPG when its gate is opened by a trigger pulse from the GTPC. The MPG is composed of several IC-shift-registers which have multi-channel outputs (twenty-four in this case). Each of the pulses from the MPG, which come out in a sequence with a time interval determined by the CPC, is used to trigger the corresponding channel of the HVPC. A high voltage pulse (with a peak voltage of$\sim$10 kV) from the HVPC triggers the TG, and as a result, the G are fired.

3. Characteristics of the camera

3.1. General

Figure 3 is a photograph of the presently constructed apparatus. Each component of the system is portable; if sufficient room is available for set-up of the apparatus, it can be used anywhere. Because the focal length of the reflector M used is 2,000 mm, the square arrays of spark gaps and the corresponding lenses* are placed at a distance of 4,000 mm from the reflector.

The internal clock pulse circuit can supply pulses with variable time

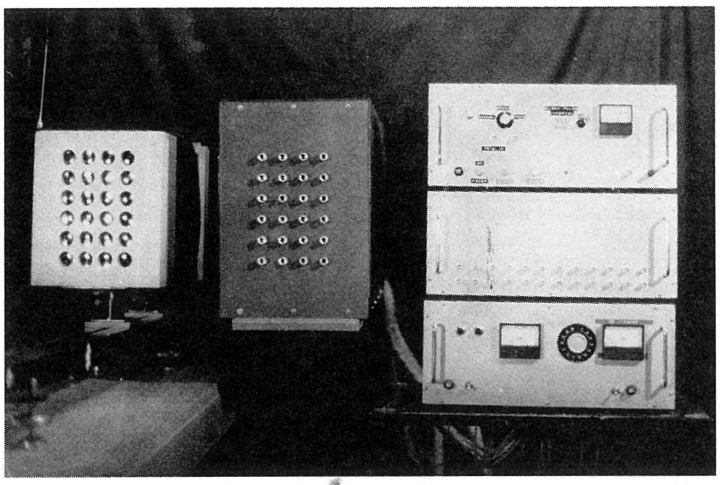

Fig. 3 The constructed apparatus, RIAM-MC1.

* Achromatic lenses with a f-number of 9.3 were used.

interval ranging from 1 μs to 999 ms by digital setting on the control panel. Clock pulses of larger interval can also be available by using an external low frequency pulse generator.

The maximum charging energy of a discharge capacitor (0.04 μF-10 kV) is 2 joules. The spark light intensity is easily controlled by changing the discharge voltage. The gap width of G is about 1 mm, which corresponds to the dimension of the light source.

3.2. Static spatial resolution

Figures 4(a) and (b) show photographs illustrating the static resolution and image linearity, respectively, of photography by the present photo-system. Two models were photographed in transmission. One was a transparent film containing a number of vertical straight lines with different intervals ranging from 4.0 mm to 0.15 mm (Fig. 4(a)). The other was a film containing many concentric circles with different diameters (Fig. 4 (b)). Figure 4(a) indicates that the highest resolution of the camera is about 0.15 mm, i.e., 6 lines/mm for the model placed at a distance of 3,000 mm from the camera lens. (A greater resolution may be obtained by exchanging the lenses for ones with a higher magnification, although the size of the largest object which can be observed will naturally be reduced.) Figure 4(b) indicates that each of the circles is well reproduced; although there

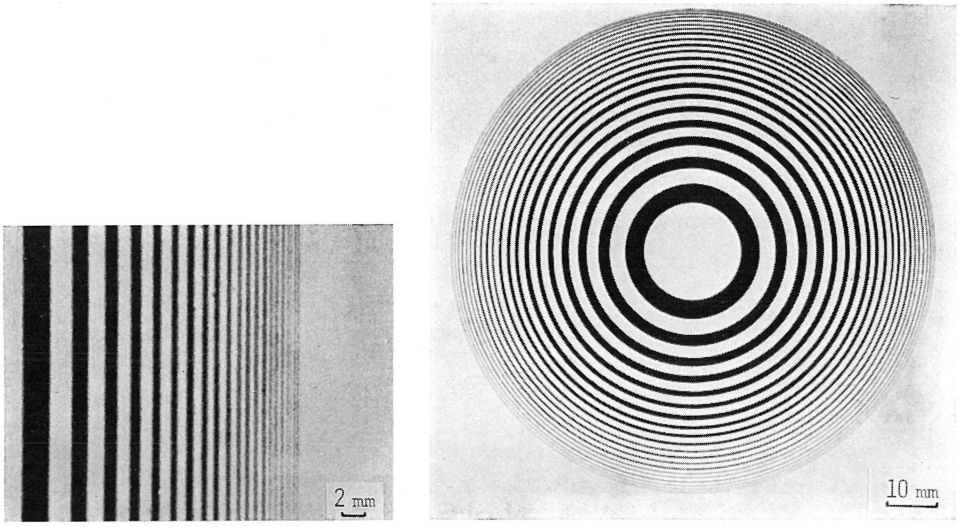

(a) (b)

Fig. 4 Photographs used to inspect the static resolution (a) and image linearity (b).

occurs a slight image contraction in the horizontal direction (approx. 0.5% in this case), this contraction may be regarded to be negligibly small.

From the results of Figs. 4(a) and (b) it may well be said that linearity of the images taken by the camera is satisfactory even for quantitative uses.

3.3. Time lags of the circuits

There inevitably occur time lags in operation of the circuits shown in Fig. 2. When the framing rate becomes higher these lags might have an influence on the accuracy of the successive spark discharge timing, as well as on the synchronization of the spark initiation with an event to be obsered. Therefore, a brief description of the circuit lags will be given here.

Figures 5(a) and (b) are typical examples of pulse traces for input (A) and output (B) of the MPG, respectively, while Fig. 5(c) shows a pulse trace for output (C) of the HVPG (see Fig. 2). For oscilloscope synchronization of the trace in Fig. 5(c), the rising part of the pulse shown in Fig. 5(b) was used; there existed a time lag of about 2.3 μs from MPG-pulse output to HVPG-pulse output. The rise time of the high voltage pulse was approx. 0.9 μs. Figure 5(d) shows the voltage waveform for the discharge capacitor on the occasion of a gap breakdown (obtained at D in Fig. 2). (The spark discharge continued for about 1.5 μs in an oscillatory manner.) Figure 5(d) indicates that there existed a time lag of roughly

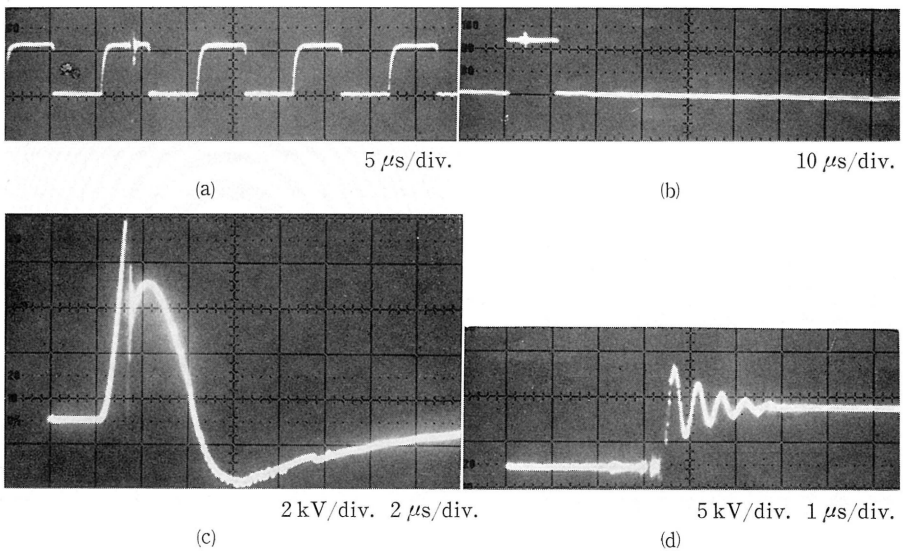

Fig. 5 Typical examples of pulse traces at A ((a)), B ((b)), C ((c)) and D ((d)) of Fig. 2.

3.2 μs from the time of the oscilloscope triggering, to the occurrence of breakdown, i.e., the breakdown at the gap in this case occurred approximately when the trigger pulse shown in Fig. 5(c) reached its maximum.

In Fig. 6 is summarized a sequence of time lags for the initial spark discharge after setting the GTPC. The total lag, $\tau_{(\text{initial})}$, consists of lags $\tau_1 \sim \tau_5$: τ_1 and τ_2 are inherent in the circuits system used; τ_1 is always smaller than one clock-pulse-interval (CPI), while τ_2 is equal to one CPI. τ_3 is 2.3 μs as shown in Fig. 5(c). The sum of τ_4 and τ_5, a discharge lag, is the time lag taken from application of a high voltage trigger pulse to initiation of the breakdown in the gap; τ_4 is the minimum vaule of the discharge lag for a given discharge condition (see Fig. 8).

It should be noted here that, while the lag τ_5 makes the spark initiation time vary for each gap, the other time lags $\tau_1 \sim \tau_4$ delay the initiation of only the first spark; therefore, they may be included as part of the delay time given by the delay circuit (DC). However, there may be some cases when presence of the time lags τ_1 and τ_2 becomes impeding in that a photograph immediately after external triggering can not be obtained. For the purpose of obtaining the "instantaneous" photograph in case of need, such a direct trigger channel, which is free from the lags τ_1 and τ_2, has been added, as is shown in Fig. 2.

As is well known[4~6], the discharge lag is not constant, but varies from shot to shot, with a distribution whose form depends on many factors, such as gap voltage (including the polarity), magnitude of the trigger pulse, gap

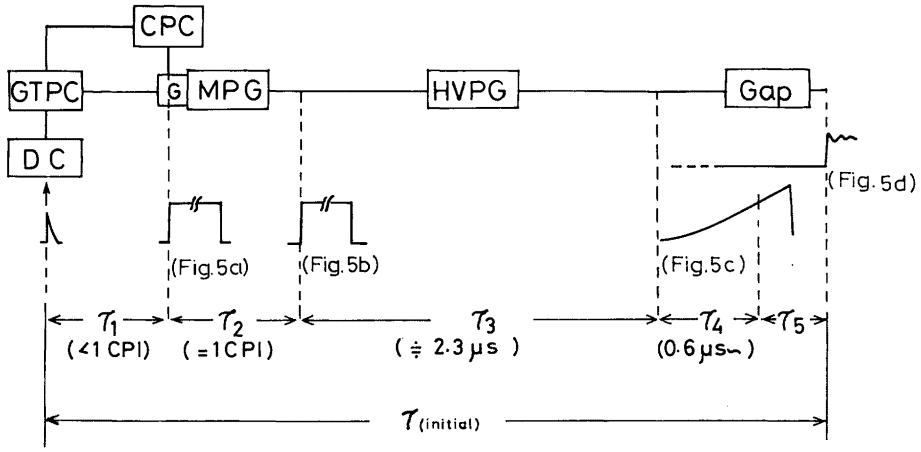

Fig. 6 The sequence of time lags for the initial spark discharge after setting the GTPC.

width, atmosphere within the gap (kind of gas, gas pressure, humidity), contamination of the gap-electrode surface, etc. In the present apparatus were used atmospheric gaps with semi-fixed widths, which were adjusted so that the static breakdown voltage (E_s) was typically in the range of $-7.5\sim -8.5$ kV.

In usual applications of the camera the time interval between light pulses is always monitored with a Si photo-diode, so that no problem occurs as to the timing identification, or velocity measurement, of an observed event, so long as the framing rate is not so high that the fluctuation of τ_s exceeds one CPI.

3.4. Characteristics of the triggered gap

For ease in operation of the camera, it is necessary that stable performance of the TG be maintained without a notable increase in the fluctuation of the discharge lag, even when the gap voltage is varied within a range of approx. 3 kV for the purpose of regulating light intensity; that is, there must be an ample range of controllability in a diagram showing the characteristic relationships between the gap width (d), the static breakdown voltage (E_{sb}), and the trigger threshold voltage (E_t). In Fig. 7 is given an example of the d-E_{sb}-E_t-characteristics, which shows that there is a voltage margin of about 4 kV between E_{sb} and E_t for a specific value of the gap width (d) taken in a usual operational range. A typical example

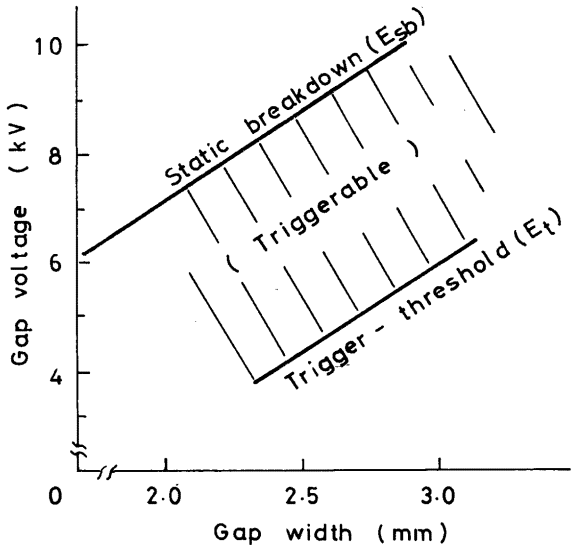

Fig. 7 An example of the d-E_{sb}-E_t-characteristics of the TG.

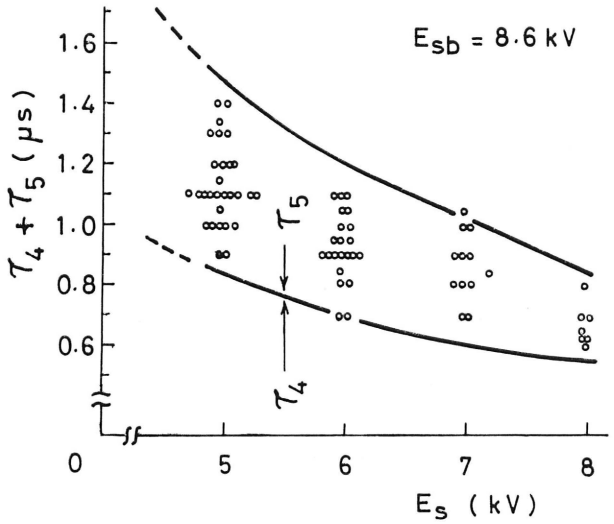

Fig. 8 A typical example of the discharge-lag of spark gap breakdowns.

of the discharge-lag distribution is shown in Fig. 8. A general tendency characteristic of spark gap breakdown is also discernible from Fig. 8; when the static gap voltage E_s is reduced without a change in the gap width the average discharge lag, as well as its fluctuation, is increased. However, it should be noted that the maximum value of τ_5 did not exceed 1.0 μs, but was usually confined to a range centered near 0.5 μs for values of E_s normally used with the present apparatus ($|E_s|>5$ kV).

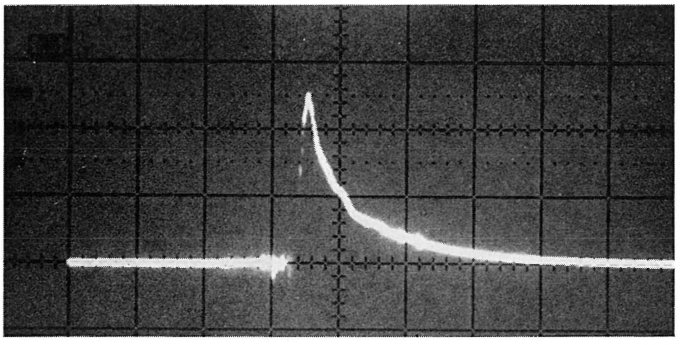

1 μs/div.

Fig. 9 An example of a light pulse trace.

3.5. Duration of the light pulse

An example of a light pulse trace, obtained with a fast response Si photodiode (HAMAMATSU, S1188-01), is illustrated in Fig. 9, which indicates that the approximate duration of the light pulse was about 0.4 μs (full width of half maximum, t_h).*

3.6. Maximum framing rate

From the fact that the fluctuation of τ_5, as well as the light pulse duration, limits the maximum possible framing rate, the results of Fig. 8 are of importance in considering the camera performance at a much higher framing rate.** If τ_5 is smaller than 0.5 μs and τ_4 is almost the same for all gaps, there occurs no confusion in the sequence of successive breakdowns at 24 spark gaps, even when triggered at a rate of 2×10^5 frames/s. Although the data obtained is not sufficient to confirm this assumption, it may be fairly asserted that, with a "safety factor" of 2, all gaps can be fired in a regular succession if they are triggered at a rate of 1×10^5 frames/s. This assertion is reasonable, because all triggered-gap elements were similarly fabricated and adjusted for a certain breakdown voltage.

As to the light pulse duration, if we assume that the reciprocal of t_h gives the maximum rate at which light pulses in a sequence can be discriminated from each other, the results for t_h described in the previous section also assures a maximum framing rate of at least 1×10^6 frames/s.

4. Some photography examples

Performance of the camera has been tested in practice at several framing rates. Some examples are shown here. Figure 10 shows an example of cavitation as well as shock propagation in a liquid caused by underwater sparking. In Fig. 11 are shown shadowgraphs of propagating waves under water produced by wire explosion. Figure 12 shows fracture shadowgraphs of PMMA, which were taken at a framing rate of 1×10^5 frames/s. Figure 13 is an example of "low-speed" photography. A series of photographs showing profile change of erupted water was taken at a framing rate of 1×10^2 frames/s. The eruption was caused by underwater sparking.

---

* Because the light pulse measurement was performed on an oscilloscope, whose input connection was miss-matching, the real pulse trace would be a little more narrow-shaped than the one shown in the Figure.

** Because τ_4 should be almost common to all gaps, it only retards the initiation of breakdown of all gaps for a certain amount of time, and does not disturb the breakdown sequence.

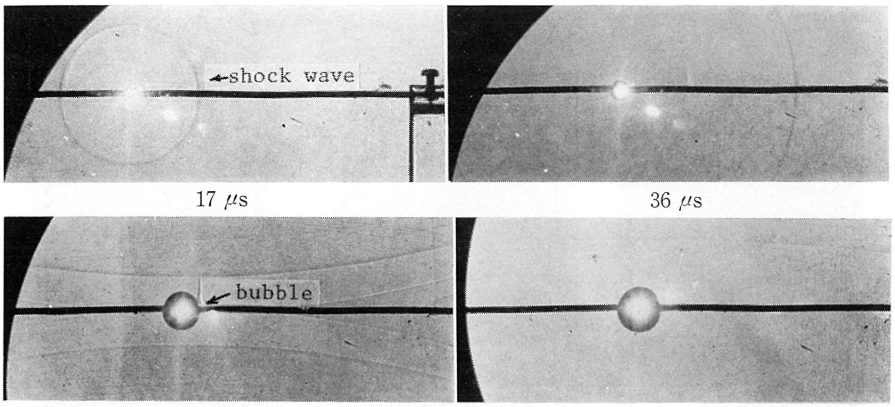

17 μs 36 μs

200 μs 360 μs

Fig. 10 Cavitation and shock propagation caused by underwater sparking (5×10^4 frs/s).

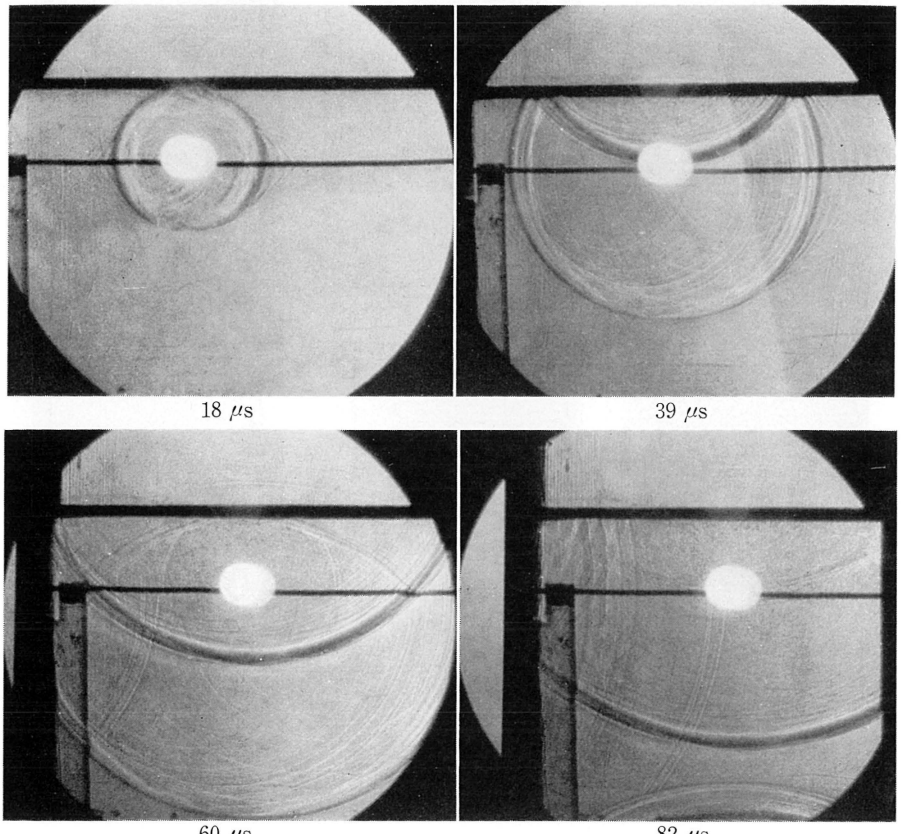

18 μs 39 μs

60 μs 82 μs

Fig. 11 Shadowgraphs of propagating water waves produced by a wire explosion (5×10^4 frs/s).

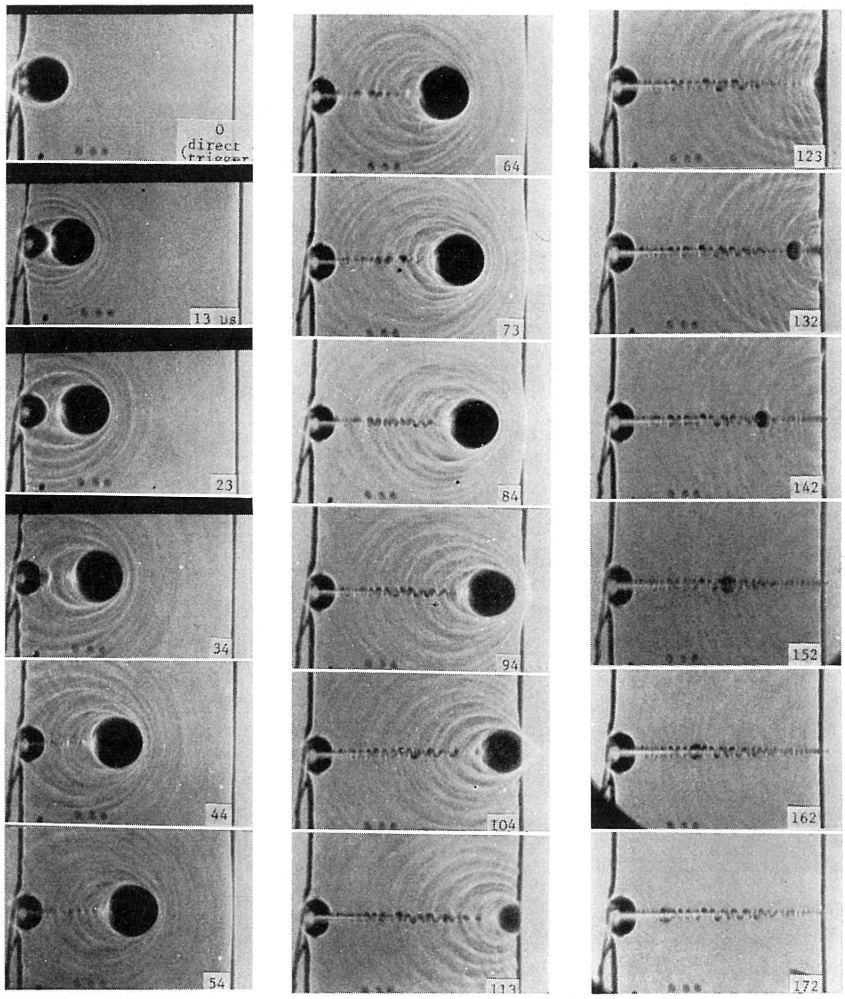

Fig. 12 Fracture shadowgraphs of PMMA (1×10^5 frs/s).

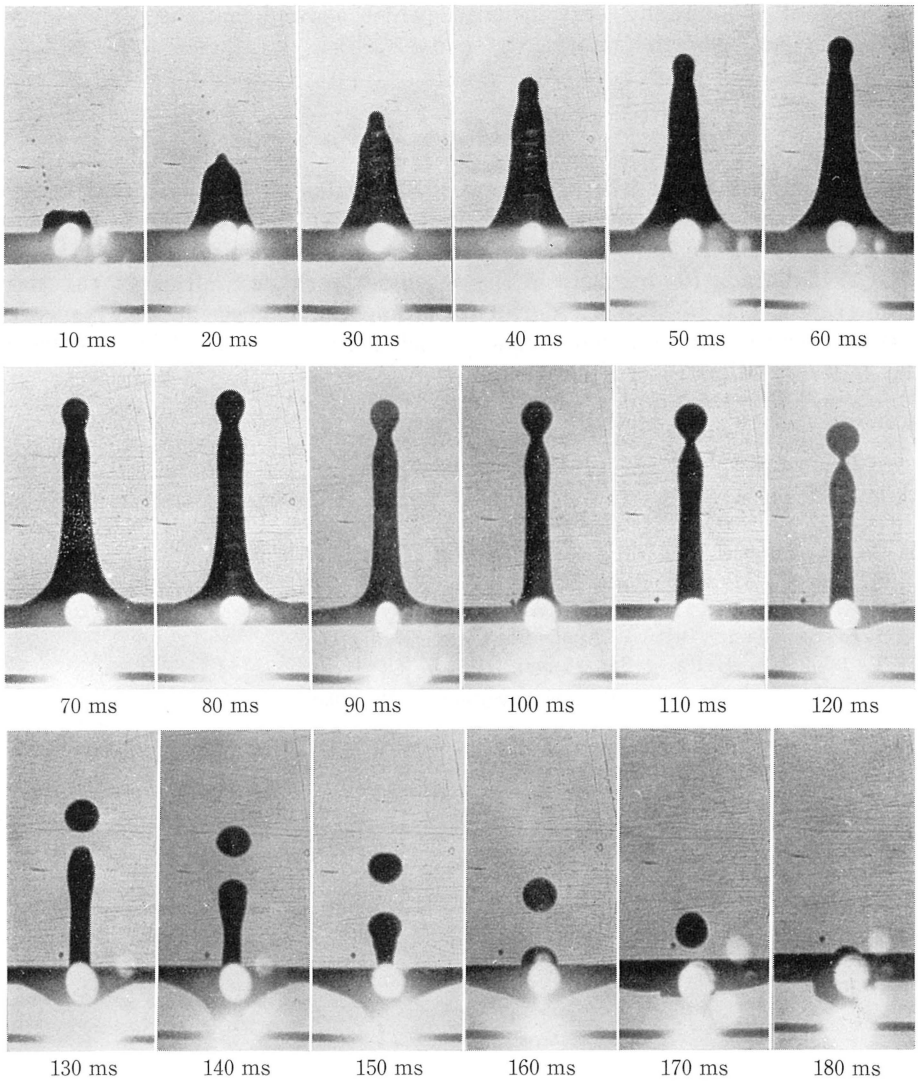

Fig. 13 An example of low speed photography (1×10^2 frm/s), showing a sequential profile change of erupted water.

5. Conclusions

An ultra-high speed camera of a pulse-controlled, multi-spark type with 24 frames has been successfully constructed. The maximum possible framing rate was 1×10^6 frames/s, whereas the minimum rate was unlimited. The full width at half-maximum duration of light pulses was 0.4 μs. Several

examples of photography were included, which showed that the performance of the camera was satisfactory.

Acknowledgements

The authors would like to express their thanks to Prof. T. Suhara for his encouragement during the course of this work, and to Prof. S. Itoh for his dicussion on the light pulse measurement. They also owe thanks to Mr. Y. Sakurada for his help in the machine work as well as in the test photography, and to Miss T. Morita for typing the manuscript. This work was performed under a Grant-in-Aid for Scientific Research (1979-1980) from the Japanese Ministry of Education.

References

1) R.E. Rowlands, C.E. Taylor and I.M. Daniel, Experimental Mechanics, *9*, 385 (1969).
2) C. Cranz and H. Schardin, Zeits. f. Phys., *56*, 147 (1929).
3) A. Stenzel, Wehrtechnische Monatshefte, No.6/7, 289 (1962).
4) G.A. Theophanis, Rev. Sci. Instr., *31*, 427 (1960).
5) T.E. Broadbent, Brit. J. Appl. Phys., *8*, 37 (1957).
6) T. Ishikawa, J. Phys. Soc. Japan, *19*, 367 (1964).

(Received September 30, 1980)